Magnetic Resonance Imaging *Versus* Computed Tomography in the Evaluation of Soft Tissue Tumors of the Extremities

ALFRED E. CHANG, M.D.,* YVEDT L. MATORY, M.D.,* ANDREW J. DWYER, M.D.,† SUVIMOL C. HILL, M.D.,† MARY E. GIRTON, R.T., SETH M. STEINBERG, PH.D.,‡ RICHARD H. KNOP, M.D., PH.D.,† JOSEPH A. FRANK, M.D.,† DAVID HYAMS, M.D.,* JOHN L. DOPPMAN, M.D.,† and STEVEN A. ROSENBERG, M.D., PH.D.*

Twenty patients with extremity soft tissue tumors were prospectively evaluated with magnetic resonance imaging (MRI) and computed tomography (CT) scans with subsequent anatomic correlation of surgical findings. MRI and CT had a similar percentage of accuracy in assessing tumor relationship with major neurovascular (80% and 70%, respectively) and skeletal (80% and 75%, respectively) structures. MRI was significantly better than CT in displaying contrast between tumor and muscle when using the T2 weighted spin echo (SE) ($p_2 < 0.002$) and inversion recovery (IR) ($p_2 < 0.005$) pulse sequences. MRI and CT were comparable in demonstrating contrast between tumor and fat. The contrast between tumor and vessel was better displayed by MRI compared with CT when using the T1 weighted SE ($p_2 < 0.001$) and T2 weighted SE ($p_2 < 0.001$) pulse sequences. T1 and T2 values were measured on fresh tumor and normal tissue samples and were used to predict relative contrast on different MRI pulse sequences using isosignal contour plots. MRI appears to offer several advantages over CT in the evaluation of extremity soft tissue tumors.

From the Surgery Branch, National Cancer Institute, Department of Diagnostic Radiology Clinical Center,† Biostatistics and Data Management Section,‡ National Cancer Institute, National Institutes of Health, Bethesda, Maryland*

MAGNETIC RESONANCE IMAGING (MRI) is a new imaging modality that does not require the use of ionizing radiation. Clinical MRI produces images based on the magnetic properties of tissues rather than their radiodensity. Computed tomography (CT) has been considered the standard diagnostic test in staging and evaluating the anatomic location of soft tissue tumors of the extremities.[1,2] As with all diagnostic imaging, the fundamental problem in evaluating soft tissue tumors of the extremities is accurate delineation between the tumor and the adjacent normal tissues. The advent of CT brought considerable advantage over more traditional modalities by more accurate display of relative radiodensities and tomographic geometry. This provided good delineation of the tumor's margins with fat, bone marrow, and cortex due to differences in radiodensity between fat, nonfatty soft tissues, bone cortex, and calcification. However, the contrast between tumor and muscle commonly remains poor and their interfaces obscure. In addition, CT is also subject to "streak artifacts" emanating from clips and bone/soft tissue interfaces. There is limited information regarding the use of MRI in the evaluation of soft tissue tumors of the extremities.[3-11] Since the magnetic properties differ considerably among tumor, muscle, and fat, MRI may offer advantages over CT in imaging tumor from adjacent normal structures.[12-16] This study was performed to determine how MRI compares with CT in the evaluation of extremity soft tissue tumors. Anatomic relationships of tumor to neighboring vital structures were determined by both MRI and CT studies prospectively and correlated with surgical findings. Contrast between tumor and adjacent normal tissues were subjectively graded for each study. In addition, T1 and T2 values were measured from normal and pathologic excised fresh tissue, which provided information regarding appropriate pulse sequences for MR imaging purposes. A brief review of fundamental MRI principles is also presented.

Materials and Methods

Patients

Twenty patients with soft tissue tumors of the extremities from the Surgery Branch, National Cancer Institute were evaluated with preoperative CT and MRI exami-

Reprint requests and correspondence: Alfred E. Chang, M.D., Surgery Branch, National Cancer Institute, Building 10, Room 2B42, Bethesda, MD 20892.

Submitted for publication: November 17, 1986.

TABLE 1. *Tumor Relationship to Major Neurovascular and Skeletal Structures*

Patient	Site	Tumor Histology	CT		MRI		Surgery	
			N/V	Bone	N/V	Bone	N/V	Bone
1	Thigh	High-grade MFH	−	−	−	−	+	+
2	Thigh	Low-grade liposarcoma	−	−	+	−	−	−
3	Leg	Benign schwannoma	−	−	+	−	+	−
4	Thigh	Low-grade neurofibrosarcoma	+	−	+	−	+	−
5	Thigh	Low-grade liposarcoma	−	+	−	+	−	+
6	Knee	Desmoid	+	−	+	−	+	+
7	Forearm	High-grade spindle cell sarcoma	−	−	−	−	−	−
8	Thigh	High-grade liposarcoma	+	−	+	−	+	−
9	Thigh	High-grade synovial cell sarcoma	+	+	+	+	+	+
10	Thigh	Low-grade liposarcoma	−	−	−	−	−	−
11	Thigh	High-grade synovial cell sarcoma	−	−	−	−	−	−
12	Groin	High-grade synovial cell sarcoma	+	+	+	−	+	−
13	Thigh	Low-grade liposarcoma	−	−	−	−	−	−
14	Thigh	High-grade synovial cell sarcoma	+	+	+	+	+	+
15	Thigh	Low-grade liposarcoma	+	−	+	−	+	−
16	Thigh	High-grade MFH	+	+	+	+	+	+
17	Arm	Desmoid	+	+	NS	NS	−	−
18	Buttock	High-grade unclassified sarcoma	+	+	+	−	−	−
19	Knee	High-grade synovial cell sarcoma	−	+	NS	NS	−	−
20	Thigh	High-grade MFH	+	+	+	+	+	+
Accuracy (%)			16/20 (80)	15/20 (75)	14/20 (70)	16/20 (80)		

N/V = neurovascular structures.
MFH = malignant fibrous histiocytoma.
(−) = no abuttment.
(+) = abuttment.
NS = not seen.

nations. The location of these tumors included 18 in the lower extremities and two in the upper extremities (Table 1). Pathologic diagnosis of these tumors are also listed in Table 1 and include 11 high-grade sarcomas, six low-grade sarcomas, two extra-abdominal desmoids, and one benign schwannoma. Histopathologic grading of the sarcomas was performed using the criteria described by Costa et al.[17] Surgery involved either amputation or wide excision of the tumor except for the schwanomma, which was removed by a marginal excision.

Anatomic Relationships

An assessment of whether the tumor was abutting or contiguous with a major neurovascular or skeletal structure was made before surgery by a designated radiologist who interpreted the CT (S. H.) or MRI (A. D.) scans. Neither individual had knowledge of the results of the other study. Correlation was then made with the surgical findings. Accuracy of each study was determined by calculating (number of correct tests/total number of tests) × 100 to yield a percentage.

Contrast Between Tumor and Normal Tissue

Image contrast between tumor and normal muscle, fat, and blood vessel was subjectively assessed on a 0–3 scale. Zero represented no contrast, 1 = minimum, 2 = intermediate, and 3 = maximum. Degree of contrast was evaluated for the CT scan and all MRI pulse sequences. Comparison of CT and each MRI pulse sequence image contrast was performed by subtracting scale score of MRI from the corresponding CT score and analyzed using a Wilcoxon paired test (one-sample). All reported p values are two-sided.

MRI and CT Imaging

Magnetic resonance images were obtained on a 0.5-tesla (21.3 MHz) super-conducting magnet (Picker International, Highland Heights, Ohio). An elliptical body coil was used with a 52 × 35-cm amperature. Spin echo (SE) and inversion recovery (IR) pulse sequences were used to obtain images in the transverse, coronal, and sagittal planes. SE images were obtained using an echo time (TE) of 26, 40, 80, or 120 msec and a repetition time (TR) of 500–2500 msec. The IR images were obtained with a TR of 1500 or 3000 msec and inversion time (TI) of 100 msec or 600 msec and a TE of 30–40 msec. In all cases, two to four repetitions were used and 128 views were obtained. Images were obtained in 10-mm contiguous slices with field of views varying between 30 and 45 cm. The average time for data collection was approximately 4.5–17.8 minutes per sequence. All images were reconstructed using a

two-dimensional Fourier Transform Algorithm and displayed on a 256 × 256-image matrix. CT scans were obtained using a General Electric CT/T 8800 or 9800 scanner (General Electric, Milwaukee, WI). Contiguous 1-cm slices were obtained to cover the entire lesion.

Tissue Relaxation Times

Tissue proton spin-lattice and spin-spin relaxation times were measured at room temperature (23.7 C) using a pulse spectrometer with a permanent magnet operating at 0.25 tesla (10.7 MHz) (Praxis II, Praxis Corporation, San Antonio, TX). Spin-lattice (T1) relaxation times were measured using a repetitive 90°–90° radiofrequency pulse. Spin-spin relaxation times (T2) were determined using an SE pulse sequence (90°–180°) radiofrequency pulse. T1 and T2 values were computed from the slope of log (Mo/Mt) *versus* time. Measurements were made within 2 hours of surgery. In all cases, three determinations of the relaxations were obtained and reported as the mean value.

Results

Assessment of Tumor Relationship with Major Neurovascular and Skeletal Structures

Table 1 lists the interpretations of CT and MRI regarding the abuttment of tumor to adjacent vital structures. Anatomic correlation was confirmed by the findings at surgical excision (Fig. 1). CT identified tumor in all patients. In two cases, the tumor was not seen by MRI. These two cases were the smallest tumors in the series, each measuring 2 cm in greatest dimension. In calculating percentage of accuracy, these two cases were considered as being incorrect for the MRI interpretation. CT and MRI had an accuracy rate of 80% and 70%, respectively, in determining abuttment to the major neurovascular structures and were not significantly different. Also, CT and MRI were equivalent in determining contiguity to bone with an accuracy rate of 75% and 80%, respectively.

Tumor Contrast to Normal Tissues

Table 2 lists the relative contrast determination between tumor *versus* muscle, tumor *versus* fat, and tumor *versus* vessel as seen on CT and the various MRI pulse sequences. Figures 1 and 2 illustrate the subjective estimates of contrast that were made. In Figure 1, patient 14 had a large synovial cell sarcoma of the left proximal thigh. On CT scan, the contrast between tumor and muscle was zero. Tumor was better distinguished from muscle on the T1-weighted SE (SE 550/26) sequence where contrast between tumor and muscle was graded as intermediate. The coronal views of the MRI in this case demonstrated the enhanced contrast between tumor and muscle on the T2-weighted SE (SE 2500/120) and IR (IR 1500/100) pulse sequences compared with the T1-weighted SE image. Another patient, illustrated in Figure 2, demonstrated similar findings. The patient had a low-grade myxoid liposarcoma of the right midthigh. On CT scan the lesion was adequately distinguished from adjacent muscle and fat. The T2-weighted SE (SE 2500/120) image demonstrated the greatest contrast between tumor and muscle with good contrast against fat. The T1-weighted IR (IR 2500/600) image showed the tumor to be dark relative to adjacent structures with greatest tumor/fat contrast.

Analysis of the contrast data between tumor to muscle, fat, and major vessels was performed. For every patient the CT contrast value was compared with the contrast values of each MRI pulse sequence. For each comparison, a ranking was assigned and an analysis performed for the entire group of patients using a Wilcoxon paired test. For tumor to muscle contrast, T2-weighted SE and IR pulse sequences were significantly better than CT ($p2 < 0.002$ and $p2 < 0.005$, respectively). Analysis of the MRI pulse sequences alone revealed that T2-weighted SE images were better than T1-weighted SE images ($p2 < 0.008$) in demonstrating tumor to muscle contrast. For tumor to fat contrast, there was no significant difference between CT and any of the MRI pulse sequences. IR images demonstrated more tumor to fat contrast compared with T1- or T2-weighted SE images ($p2 = 0.03$ and 0.04, respectively). For tumor to vessel contrast, T1- and T2-weighted SE images were significantly better than CT (each, $p2 < 0.001$). T1- and T2-weighted SE pulse sequences were significantly better than the IR pulse sequence in demonstrating tumor to vessel contrast ($p2 = 0.005$ and $p2 < 0.004$, respectively).

T1 and T2 Tissue Determinations

Table 3 lists the T1 and T2 determinations measured on fresh tissue removed at surgery from 13 patients. Each value is the average of at least three determinations made on each sample. The average T1 value of all tumor samples was greater than muscle, fat, and skin. The average T2 value of all tumor samples was also greater than muscle and skin but was identical to fat. There were no significant differences between T1 and T2 values for low-grade and desmoid tumors *versus* high-grade tumors.

In Figure 3, T1 and T2 values for each tissue specimen have been plotted on isosignal contour curves that are mathematically generated using the technique described by Kurtz and Dwyer.[18] The signal strength of an MR image depends on a variety of factors that include T1 and T2 tissue values as well as the pulse sequence. Theoretical isosignal curves can be constructed for any pulse sequence and will display topographically the relationship of signal

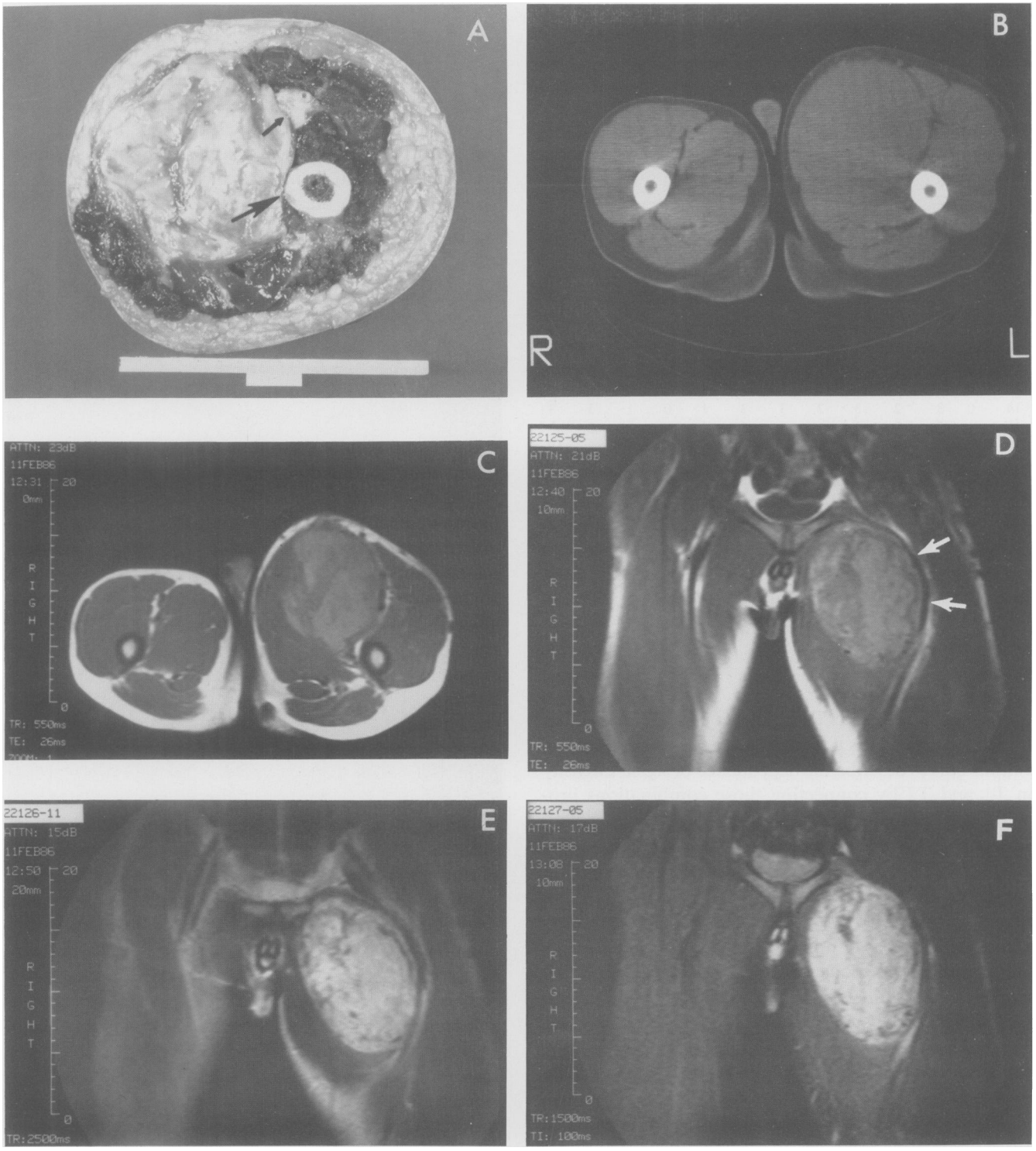

FIGS. 1A–F. Patient 14 with a high-grade synovial cell sarcoma of the left proximal thigh requiring a hemipelvectomy. *A.* Cross-section through midportion of the tumor that revealed abuttment to femur (large arrow) and the femoral neurovascular bundle (small arrow). *B.* CT of the thigh that showed asymmetry of thigh but no demarcation between tumor and muscle. *C.* T1-weighted SE cross-section that demonstrated a distinct tumor/muscle interface and excellent tumor/fat contrast. *D.* T1-weighted SE coronal view with displacement of femoral vessel laterally (white arrows) and visualization of craniocaudal margins. *E.* T2-weighted SE coronal view that demonstrated increased tumor/muscle contrast and decreased tumor/fat contrast compared with the T1-weighted SE image. *F.* The IR 100 pulse sequence that also showed superior tumor/muscle and equivalent tumor/fat contrast compared with the T1-weighted SE image.

TABLE 2. *Tumor Contrast to Adjacent Normal Tissues*

	Tumor/Muscle				Tumor/Fat				Tumor/Vessel			
		MRI				MRI				MRI		
Patient	CT	IR	T1*	T2†	CT	IR	T1*	T2†	CT	IR	T1*	T2†
1	1	0	3	3	2	3	1	1	1	0	2	3
2	3	3	3	3	0	0	0	0	3	3	3	3
3	1	3	0	ND	1	3	3	ND	1	3	3	ND
4	1	3	2	3	2	3	3	1	1	0	2	3
5	2	2	2	3	0	1	0	2	2	1	1	3
6	1	3	ND	2	3	0	ND	1	0	0	ND	2
7	1	3	3	3	2	1	0	1	0	0	3	3
8	1	3	3	3	2	3	3	3	1	0	3	3
9	0	1	1	3	3	2	0	2	0	1	3	1
10	2	2	2	3	2	3	0	2	2	0	3	3
11	1	ND	0	2	1	ND	3	3	1	ND	1	3
12	1	0	1	2	1	2	2	1	0	1	2	3
13	0	0	NS	NS	1	1	NS	NS	0	1	NS	NS
14	0	3	2	3	2	3	3	1	0	1	3	3
15	1	3‡	0	3	1	3	3	2	1	3	3	3
16	0	3‡	0	ND	3	3	3	ND	0	2	2	ND
17	1	NS	NS	NS	1	NS	NS	NS	1	NS	NS	NS
18	0	3‡	0	ND	3	3	3	ND	0	3	2	ND
19	0	NS	NS	NS	3	NS	NS	NS	0	NS	NS	NS
20	0	3‡	0	3	3	3	3	0	0	0	3	3

* T1-weighted SE sequence.
† T2-weighted SE sequence.
‡ IR 1500/100, all other IR sequences were IR 3000/600.
ND = not done.
NS = not seen.

intensity to the T1 and T2 tissue properties. Each graph in Figure 3 represents a specific pulse sequence. Isosignal contour curves describe the dependence of signal intensity on T1 and T2 by connecting those combinations producing equal signal intensity. The number associated with each curve represents its relative signal strength on an arbitrary scale of 0.1–0.9. By plotting the actual tissue T1 and T2 values on each pulse sequence contour graph we can understand why two different tissues have relatively good contrast (*i.e.*, on different curves) on one pulse sequence and yet are isodense (*i.e.*, on the same curve) on another. For instance, the tumor to muscle contrast can be predicted to be better on the T2-weighted SE (SE 2000/800) and IR (IR 1500/100/26) pulse sequences compared with the T1-weighted SE (SE 500/40) pulse sequence. The distribution of tumor and muscle T1 and T2 values on the T2-weighted SE and IR graphs lie on different isosignal curves, indicating contrast on an MR image. However, the distribution of the tumor and muscle T1 and T2 values plotted on the T1-weighted SE graph fall generally on the same isosignal curve, indicating similar signal intensity and minimal or no contrast on an MR image. Likewise, the tumor to fat contrast would be predicted to be minimal or none on a T2-weighted SE image since the T2 values of tumor and fat are identical and would place these tissues on the same isosignal curve (see Fig. 3B).

Discussion

Since the use and interpretation of MRI are greatly facilitated by some understanding of its basic physics, a brief review of its fundamentals is presented. Clinical MRI is rooted in the magnetic properties of the hydrogen nucleus, a proton. As this is a charged spinning particle, it may be likened to a tiny bar magnet or dipole. When placed in a strong magnetic field, as in an MR scanner

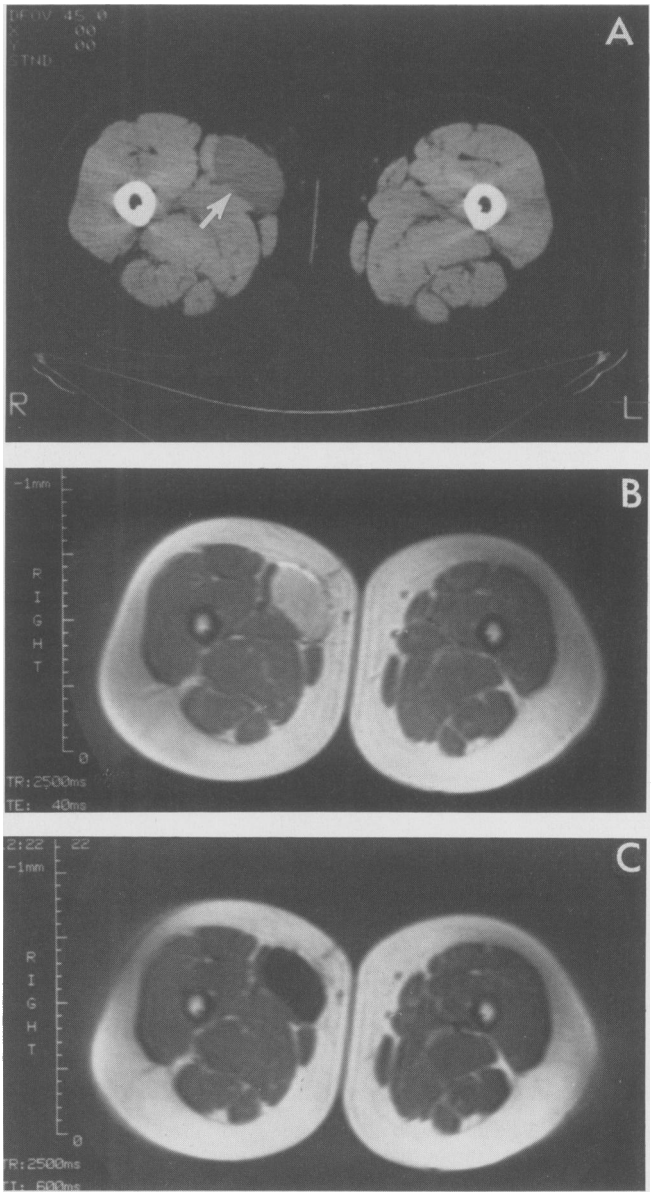

FIGS. 2A–C. Patient 10 with a low-grade liposarcoma of the right midthigh. *A.* CT of the thigh that demonstrated moderate contrast between tumor and surrounding muscle (white arrow) and fat. *B.* T2-weighted SE demonstrated the tumor to be brighter with enhanced tumor/muscle contrast compared with CT image. *C.* The IR 600 image demonstrated the tumor to be dark with good demarcation from surrounding muscle and fat.

TABLE 3. *T1 and T2 Tissue Measurements**

	Tumor		Muscle		Fat		Skin	
Tumor Histology†	T1	T2	T1	T2	T1	T2	T1	T2
High grade‡	882	80						
High grade	1248	81	610	55			380	58
High grade	900	69						
High grade	753	92	480	58				
High grade	696	80	559	68	245	82	404	72
High grade	564	80	475	50	243	69	311	30
High grade§	553	47	541	39	215	58		
	478	40						
High grade§	688	54	587	40	254	59		
	675	55						
Low grade	1570	105	530	57	245	82		
Low grade	1103	42	638	41	287	54	459	45
Desmoid	743	84			287	85		
Desmoid	652	64	547	59	291	77		
Desmoid‖	680	78						
	578	77						
Mean ± SEM	798 ± 72	71 ± 5	552 ± 18	52 ± 3	258 ± 10	71 ± 4	389 ± 31	51 ± 9

* Average of at least three separate determinations of each specimen in msec, measured at 0.25 tesla.

† All tumors are soft tissue sarcomas unless indicated otherwise.

‡ Fluid from adjacent seroma had T1 = 1380 msec, T2 = 142 msec.

§ Different tumor samples taken from large single tumor mass.

‖ Patient had two separate tumors.

(0.3–1.5 tesla in common clinical use), it assumes the motion of a gyroscope in a gravitational field and precesses about the direction of the magnetic field, the "z direction." At 0.5 tesla, used in this study, hydrogen atoms precess at 21.3 MHz; the relationship being linear with field strength. MRI is macroscopic, assessing the aggregate behavior of numerous hydrogen nuclei. Its understanding is greatly facilitated by consideration of the net magnetization vector, M, of the tissue. M is the summation of the magnetic dipoles of the individual hydrogen nuclei and, hence, is a measure of the net magnetization. It is commonly considered with respect to an x,y,z coordinate system. Z is the direction of the external magnetic field, and xy is the plane perpendicular to it. M_z and M_{xy} are the components of net magnetization along the z axis and in the xy plane, respectively.

When placed in a magnetic field, the hydrogen nuclei begin to precess about z, the direction of the magnetic field, eventually reaching equilibrium. At equilibrium, M is pointed in the z direction, M_{xy} is zero. When subjected to a radio wave oriented along the xy plane and at the precessional frequency, the individual protons acquire energy and are "excited." The aggregate result of such a so-called "excitation pulse" is reflected in the change that occurs in M. Specifically, M is rotated away from the z axis, its equilibrium position. Excitation pulses are denoted in terms of the amount of rotation they achieve. A 90° pulse rotates M from the z axis 90° onto the xy plane. Hence, as a result of this pulse, M acquires a nonzero xy component and loses its z component. This is of fundamental importance in imaging as the signal measured directly reflects the xy component. At equilibrium, it is zero and, hence, no signal is measured. After the 90° pulse there is measurable signal whose assessment and anatomic mapping constitute the formation of the MR image.

Relaxation is the opposite of excitation and represents the return to equilibrium. It comprises two processes, the loss of M's xy component and the reconstitution of the z component. These occur simultaneously but commonly at different rates. Loss of the xy component is termed transverse or spin-spin relaxation. Reconstitution of the z component of M is termed longitudinal or spin-lattice relaxation. Each occurs in an exponential fashion governed by different time constants: T1 for longitudinal and T2 for transverse. The longer the time constant, the slower the relaxation. MRI's ability to provide superior anatomic detail among soft tissues is predominantly due to their differences in relaxation times.

The link between tissues' MRI properties (most importantly, relaxation times) and the degree of contrast and anatomic detail of the image are provided by the pulse sequence. A pulse sequence is a precisely defined pattern of excitation pulses and listening times. In the production of an MR image, the pulse sequence is repeated numerous times (commonly 128–1000 times) to acquire sufficient information to produce a two-dimensional image. One pulse sequence used in this study is an SE. It consists of a 90° pulse followed by a pause, after which a 180° pulse is performed. Then, after an additional pause, the signal is assessed. After a much longer pause, the cycle is begun again. The signal intensity of a tissue in the image is dependent on its relaxation times and the

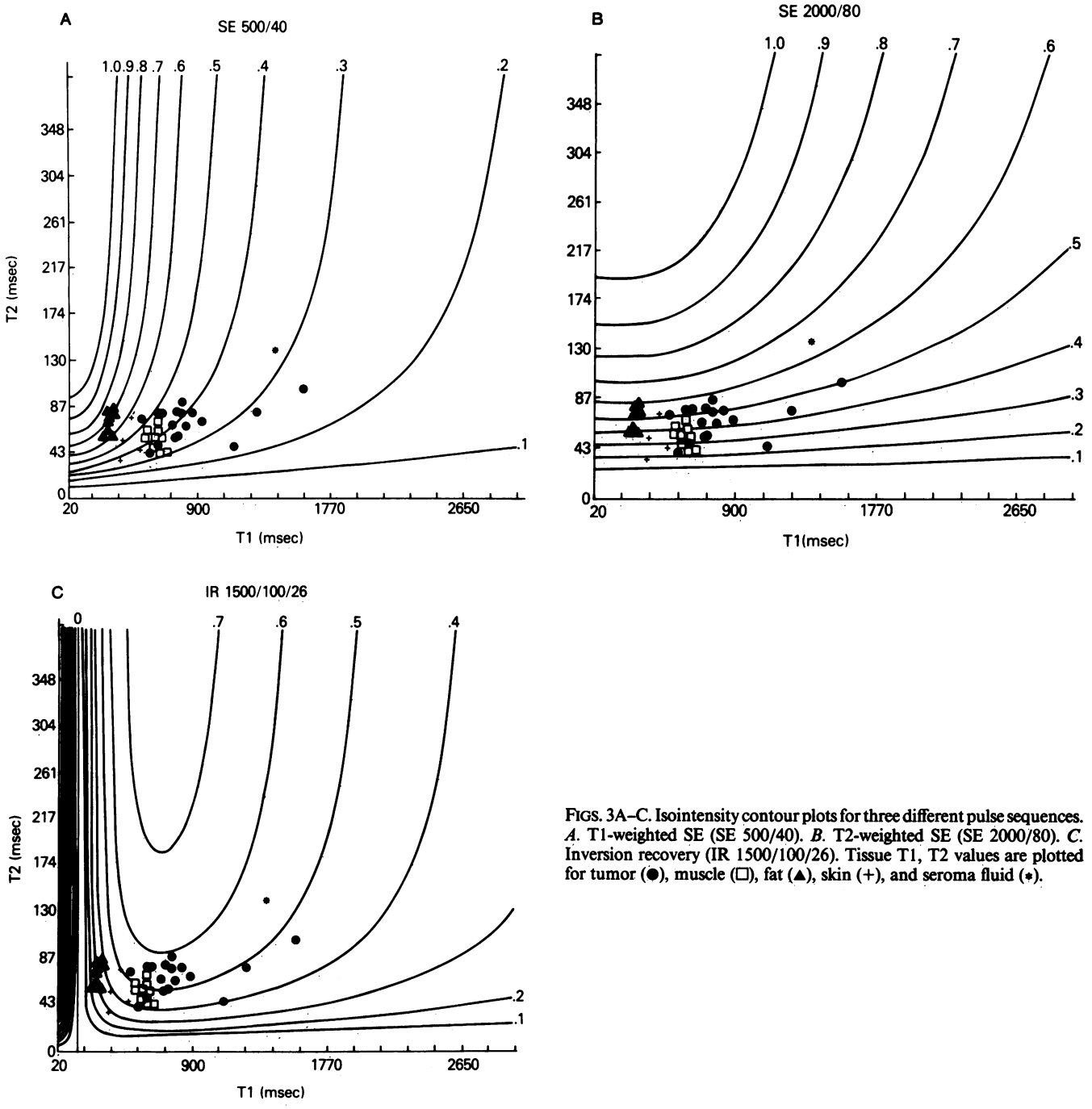

FIGS. 3A–C. Isointensity contour plots for three different pulse sequences. *A.* T1-weighted SE (SE 500/40). *B.* T2-weighted SE (SE 2000/80). *C.* Inversion recovery (IR 1500/100/26). Tissue T1, T2 values are plotted for tumor (●), muscle (□), fat (▲), skin (+), and seroma fluid (*).

duration of these pauses. Useful descriptive terms, which are common in MR parlance to describe pulse sequences, are T1-weighting and T2-weighting. A pulse sequence that is T1-weighted or T1-dependent produces signal intensities predominantly dependent on the T1 of tissues. These commonly provide good anatomic depiction as normal tissues commonly differ in T1. With T2-dependent or weighted pulse sequences, signal intensities predominantly depend on differences in T2. These are commonly held to be more sensitive to pathology, particularly in the head, as pathologic processes characteristically (but not specifically) prolong T2, providing visibility of lesions by increasing their signal intensity.

A prospective study examining the efficacy of CT and MRI in the evaluation of 20 patients with soft tissue extremity tumors was performed with surgical correlation. Our study indicated that MRI was comparable to CT in determining the relationship of tumor to adjacent vital structures. However, in two cases when tumor was small in volume, MRI could not depict masses that were seen

on CT scanning. This may be due to the decreased spatial resolution of MRI that is currently not equal to that of CT; however, we found the anatomic detail displayed by both scans to be similar. Because MRI imaging can be performed without the injection of contrast material, it may be preferable to use in patients with known allergies to contrast agents.

MRI allows for coronal and sagittal imaging, which can enable direct visualization of the extent of the tumor in the craniocaudal axis. The degree to which the addition of these images adds to the clinical evaluation of the patient is not easily quantified. We could not quantify its impact to the evaluation of the patients. Other reports suggest that those views facilitate the planning of the surgical approach.[11]

MRI was significantly better than CT in providing contrast between tumor *versus* normal muscle and vessels. The T2-weighted SE image was the best in distinguishing tumor from muscle and vessels compared with CT. Both CT and MRI were comparable in distinguishing tumor from fat. Among the MRI pulse sequences, IR was significantly better than the T1- and T2-weighted SE pulse sequences in distinguishing tumor from fat. Previous reports have recommended obtaining T1-weighted SE images to demarcate tumor from fat and T2-weighted SE images to delineate tumor from muscle.[10,11] No studies have examined IR images in a critical way. We also found that a T1- and T2-weighted SE was necessary for complete tumor delineation. In addition, the IR pulse sequence displayed excellent tumor/muscle contrast and was superior in demonstrating tumor/fat contrast compared with standard T2-weighted SE images. Preliminary results involving a variety of malignancies suggest that the short T1 IR (IR 1500/100) sequence is as effective and in some cases superior to the T2-weighted SE sequence in displaying the extent of tumor.[19]

Our data also include the determination of T1 and T2 values of tumor and normal tissues. Earlier reports suggested that the T1 and T2 values of malignant tissues *in vitro* differed from benign lesions and normal tissues, and hence may allow a specific diagnosis of malignancy.[12–14] It has also been suggested that MRI can even distinguish the histologic grade of tumors.[9] We could not make a clear distinction between high-grade soft tissue sarcomas *versus* low-grade sarcomas or benign desmoids. As shown in Figure 3, there is some overlap of T1 and T2 values between tumor and muscle. We conclude that MRI is not tissue specific for extremity soft tissue tumors except to distinguish fatty tumors. In a limited sampling, Petasnick et al. also concluded that the measurement of T1 values from excised extremity masses was not helpful in distinguishing malignant *versus* benign pathology.[11] Preliminary data involving positron emission tomography to measure glucose utilization of soft tissue sarcomas may be a more functional way to determine the degree of malignancy of these tumors.[20]

The T1 and T2 values measured in this study are helpful in predicting the appropriate pulse sequences that will yield the best contrast. These values can be plotted on isointensity contour curves that have been mathematically derived.[18] As shown in Figure 3, these curves are directly analogous to elevation lines of a topographic map or isobars on a weather map. They are graphed on a T1 (horizontal axis) and T2 (vertical axis) plane. Each tissue may be located on the plane in terms of its T1 and T2. Each line connects those combinations of T1 and T2 that would have the same signal intensity. The numbers associated with each line indicate its relative signal intensity. The ensemble of curves hence defines a signal intensity terrain. In Figure 3A, maximal signal intensities occur in the upper left-hand corner with tissues of shortest T1 and longest T2. Reduction in signal intensity is achieved by either prolongation of T1 or reduction in T2. Tissues on different isointensity lines have differing signal intensities and thus display contrast on the MR image. Tissues on the same isointensity line are unresolvable. These curves provide an analytic tool in the choice of pulse sequence. A logical choice is the pulse sequence in which the tissues to be distinguished are separated by or lie on different isointensity curves. The orientation and spacing of the lines reflects the degree and magnitude of T1-/T2-weighting. In the lower part of Figure 3B, the lines are tightly packed and horizontal. This indicates considerable T2-weighting and negligible T1-weighting since prolongation of T1 moves along the line, effecting no change in signal intensity, whereas change in T2 moves off the line onto another line, effecting a maximal change in signal intensity. The closer the lines, the stronger the weighting. Conversely, in the upper part of Figure 3A, the lines are vertically oriented, defining T1-weighting by analogous but reversed considerations. Of note are the curvilinear character of all three plots indicating a combination of both T1- and T2-weighting, save for very selected combinations of T1 and T2. Hence, the terms T1- and T2-weighting are elliptic, more properly indicating the dominant factor in a limited range of T1s and T2s.

Figures 3A and 3B demonstrate a fundamental problem in soft tissue tumor imaging. This is due to the relationship in T1s and T2s between muscle, tumor, and fat. Specifically, tumor prolongs both T1 and T2 relative to muscle. Hence, with a pulse sequence as shown in 3A in which prolongation of both T1 and T2 move along the same curve, muscle and tumor may have negligible contrast, which provided no advantage over CT. On a T2-weighted image, as shown in Figure 3B, tumor and fat may be obscure due to similar T2s. Figure 3C demonstrates an improved situation in which the isointensity contour curves are such that concomitant increases in T1 and T2

move perpendicular to the curve, achieving maximal contrast. For this study, both traditional T1 and T2 pulse sequences were as demonstrated in Figures 3A and 3B. In addition, a newer pulse sequence was used as shown in Figure 3C.

MRI has several advantages over CT as a diagnostic tool. MRI does not require ionizing radiation nor contrast agents to obtain images. It can give anatomic information in several planes: transaxial, sagittal, and coronal. Our study indicates that MRI gives comparable definition of tumor location with respect to adjacent vital structures compared with CT. Also, contrast between tumor to muscle and vessels is better than CT. The disadvantages of MRI include relative high cost and increased imaging time. To perform an adequate study, a T1- and T2-weighted SE along with an IR pulse sequence should be performed. Obtaining coronal and sagittal images further prolongs the examination time. Also, with the current technology, MRI may not detect small lesions as well as CT because of poor signal to noise ratio seen with MRI. As the technology improves, these disadvantages will no doubt be eliminated.

Acknowledgment

We thank Rosalind A. Blackwood for her invaluable secretarial help in preparing this manuscript.

References

1. Enneking WR. Preoperative staging of sarcomas. Cancer Treat Symposia 1985; 3:67–70.
2. National Institutes of Health Consensus Development Panel on Limb-sparing Treatment of Adult Soft Tissue Sarcomas, Consensus Statement. Cancer Treat Symposia 1985; 3:1–5.
3. Moon KL, Genant HK, Helms CA, et al. Musculoskeletal applications of nuclear magnetic resonance. Radiology 1983; 147:161–171.
4. Brady TJ, Rosen BR, Pykett IL, et al. NMR imaging of leg tumors. Radiology 1983; 149:181–187.
5. Scott JA, Rosenthal DI, Brady TJ. The evaluation of musculoskeletal disease with magnetic resonance imaging. Radiol Clin North Am 1984; 22:917–924.
6. Hudson TM, Hamlin DJ, Enneking WF, Petterson H. Magnetic resonance imaging of bone and soft tissue tumors: early experience in 31 patients compared with computed tomography. Skeletal Radiol 1985; 13:134–146.
7. Richardson ML, Amparo EG, Gillespy T, et al. Theoretical considerations for optimizing intensity differences between primary musculoskeletal tumors and normal tissue with spin-echo magnetic resonance imaging. Invest Radiol 1985; 20:492–497.
8. Petterson H, Hamlin DJ, Mancuso A, Scott KN. Magnetic resonance imaging of the musculoskeletal system. Acta Radiol 1985; 26: 225–234.
9. Rosenthal DI, Scott JA, Brady TJ. Magnetic resonance imaging of the extremities. Caradiovasc Intervent Radiol 1986; 8:377–381.
10. Totty WG, Murphy WA, Lee JKT. Soft-tissue tumors: MR imaging. Radiology 1986; 160:135–141.
11. Petasnick JP, Turner DA, Charters JR, et al. Soft-tissue masses of the locomotor system: comparison of MR imaging with CT. Radiology 1986; 160:125–133.
12. Damadian R. Tumor detection by nuclear magnetic resonance. Science 1971; 171:1151–1153.
13. Hollis DP, Economou JS, Parks LC, et al. Nuclear magnetic resonance studies of several experimental and human malignant tumors. Cancer Res 1973; 33:2156–2160.
14. Damadian R, Zaner K, Hor D, DiMaio T. Human tumors detected by nuclear magnetic resonance. Proc Natl Acad Sci USA 1974; 71:1471–1473.
15. Eggleston JC, Saryan LA, Hollis DP. Nuclear magnetic resonance investigations of human neoplastic and abnormal nonneoplastic tissues. Cancer Res 1975; 35:1326–1332.
16. Cameron IL, Ord VA, Fullerton GD. Characterization of proton nmr relaxation times in normal and pathological tissues by correlation with other tissue parameters. Magn Reson Imaging 1984; 2:97–106.
17. Costa J, Wesley RA, Glatstein E, Rosenberg SA. The grading of soft tissue sarcomas. Cancer 1984; 53:530–541.
18. Kurtz D, Dwyer A. Isosignal contours and signal gradients as an aid to choosing MR imaging techniques. A Comput Assist Tomogr 1984; 8(5):819–828.
19. Frank JA, Dwyer AJ, Sank VJ, et al. The short T1 inversion recovery pulse sequence for the detection and delineation of malignancy: a comparison to the T2 dependent spin-echo pulse sequence. Proc Soc Magn Reson Med 1986; 4:1332–1333.
20. Kern KA, Brunetti A, Norton JA, et al. Prediction of tumor grade in human extremity sarcomas by positron emission tomography. Submitted for publication.